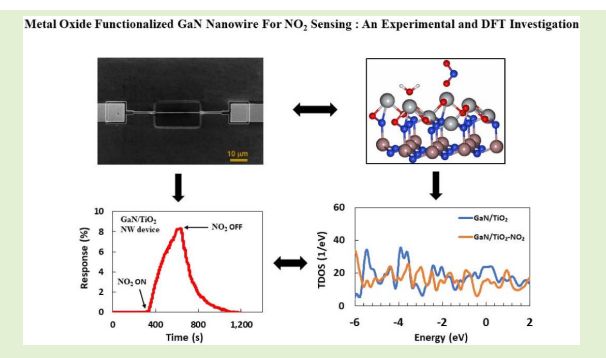


Functionalization of GaN Nanowire Sensors With Metal Oxides: An Experimental and DFT Investigation

Md Ashfaque Hossain Khan[®], Brian Thomson, Abhishek Motayed, Qiliang Li, and Mulpuri V. Rao

Abstract—The detection of NO₂ molecules by GaN nanowire sensors which were functionalized with various metal oxides have been comprehensively studied with device fabrication, characterization and modeling with first-principles calculations based on density functional theory (DFT). In this work, GaN nanowires were prepared on Si substrate by standard top-down fabrication process and then fabricated into resistor based chemical sensors. The surface of GaN nanowires were functionalized by three metal oxides: TiO₂, ZnO and SnO₂ for analysis. The UV illuminated device characterization results indicated that the devices with TiO₂ functionalization exhibited the highest response toward NO₂ gas. It showed quick response (240s) and recovery (280s)



process with strong NO₂ selectivity. In modeling, the oxide functionalized GaN in contact with NO₂ molecule was designed and geometrically optimized. Simulation results indicated that TiO₂ functionalization enabled the most energy favorable surface for NO₂ adsorption among the three metal oxides. In addition, the electronic properties of these oxide functionalized GaN have been studied in terms of the total density of states (TDOS) and projected density of states (PDOS), indicating an excellent agreement with the above-mentioned experimental measurements. Furthermore, the effect of environmental humidity on the adsorbate-nanocomposite interaction has been simulated and studied. Overall, the metal oxide functionalization significantly enhances the performance of GaN gas sensors and selecting an appropriate oxide will optimize the detection.

Index Terms—Gas sensor, GaN nanowire, metal oxide, nitrogen dioxide (NO₂), density functional theory (DFT), density of states.

I. INTRODUCTION

Compound semiconductors are mostly synthesized from elements in groups II to VI of the periodic table. Among the group III-Nitride semiconductor materials, bulk GaN has been highly explored for various applications such as- optoelectronic devices [1], electronic devices [2], biosensors [3], chemical sensors [4] and so on. Having a direct wide band gap of 3.4 eV at room temperature, GaN is chemically

Manuscript received January 19, 2020; revised February 29, 2020; accepted March 1, 2020. Date of publication March 4, 2020; date of current version June 4, 2020. This work was supported by NSF under Grant ECCS1840712. The associate editor coordinating the review of this article and approving it for publication was Dr. Yong Zhu. (Corresponding authors: Md Ashfaque Hossain Khan; Qiliang Li; Mulpuri V. Rao.)

Md Ashfaque Hossain Khan, Qiliang Li, and Mulpuri V. Rao are with the Department of Electrical and Computer Engineering, George Mason University, Fairfax, VA 22030 USA (e-mail: mkhan53@gmu.edu; qli6@gmu.edu; rmulpuri@gmu.edu).

Brian Thomson and Abhishek Motayed are with N5 Sensors, Inc., Rockville, MD 20850 USA.

This article has supplementary downloadable material available at http://ieeexplore.ieee.org, provided by the authors.

Digital Object Identifier 10.1109/JSEN.2020.2978221

very much robust, very attractive for application in harsh environment. It possesses high electron mobility, high heat capacity, good thermal conductivity and high breakdown voltage [5]. By possessing large surface-to-volume ratio, nanostructures such as nanowires, nanorods, nanotube, nanoparticles and nanobelts offer high performance chemical sensing [6]. The electronic properties of quantum confinement of electrons within GaN nanostructures lead to various electronic [7] and optical applications [8].

Metal oxide-based sensors to detect the environmental pollutants have been the subject of intense research for several decades [9]. However, metal-oxide sensors lack precise selectivity towards any specific gas. The mechanism of sensing involves chemical interaction of the analyte with the oxygen chemisorbed on the surface [10]. Also, they suffer from high power requirement and unstable operation at harsh environmental conditions. GaN/metal-oxide nanostructured devices have the potential to address these sensing limitations. Furthermore, selectivity of the sensor can be improved by employing several techniques [11]–[13], including sensor array [14] and Back-gate Field Effect Transistor (FET) sensor [15], [16].

1558-1748 © 2020 IEEE. Personal use is permitted, but republication/redistribution requires IEEE permission. See https://www.ieee.org/publications/rights/index.html for more information.

The metal-oxide nanoparticles can increase the adsorption of chemical species by introducing additional adsorption sites, thus increasing the sensitivity of GaN/metal-oxide based sensor [17]. Sensor current modulation can be achieved as well through the formation of a nanosized depletion region between GaN nanostructure and metal-oxide depending on the analyte adsorption [18]. Moreover, the metal or metal-oxide nanoparticles can act as catalysts to enhance spill-over phenomena of radicals over semiconductor [19].

Anatase phase titanium dioxide (TiO₂) has attracted great attentions due to its excellent properties such as high catalytic efficiency and large band-gap, long-term stability, low cost and non-toxicity [20]. These characteristics make TiO₂ as one of the suitable candidates for high performance gas sensing material. ZnO exhibits wurtzite crystal structure with a band gap energy of 3.37 eV. Also, it is less toxic, available in diverse morphologies, optimally conductive, quiet stable, and inexpensive [21]. All these properties make ZnO appropriate for using in chemical sensing applications. SnO₂ is one of the most extensively studied metal oxides in gas sensing applications [22]. It promotes the adsorption of atmospheric oxygen onto its surface due to possessing non-stoichiometry and thus, become sensitive towards toxic gases [23].

Nitrogen dioxide (NO₂) is one of the common toxic air pollutants, mostly found as a mixture of nitrogen oxides (NO_x) with different ratios (x). The LC₅₀ (the lethal concentration for 50% of those exposed) for one hour of NO₂ exposure for humans has been estimated as 174 ppm [24]. The major sources of NO₂ are from combustion of fuels such as certain coals and oil [25], biomass burning due to the extreme heat of lightning during thunderstorms [26], and nitrogen fixation by microorganisms due to agricultural fertilization [27]. The noteworthy impacts of NO₂ include: respiratory inflammation of the airways, decreased lung function due to long-term exposure, increased risk of respiratory conditions [28], increased responsiveness to allergens, contribution to the formation of fine particulate matter (PM) and ground level ozone which have adverse health effects, and contribution to acid rain causing damage to vegetation, buildings and acidification of lakes and streams [29]. So, precise detection of such an injurious molecule is vital to public health and environmental protection.

There have been a few computational studies on the adsorption behavior of cluster-assembled and two-dimensional GaN [30]–[32]. However, the computational analyses of metal-oxide functionalized GaN nanocomposites have not yet been reported to best of our knowledge. In this paper, we studied NO₂ gas sensing properties of GaN nanowire-based sensors functionalized with various metal-oxides. To further verify the experimental results, adsorption behaviors of NO₂ molecules on those metal-oxide/GaN nanocomposites have been investigated via density functional theory (DFT) based on first principles. Primarily, promising metal-oxides for gas sensor applications such as, TiO₂, ZnO and SnO₂ have been considered as functionalizing materials on GaN. Depending on target analyte molecules, many other catalytic metal-oxides can be explored to achieve outstanding adsorption characteristics.

II. EXPERIMENTAL DETAILS

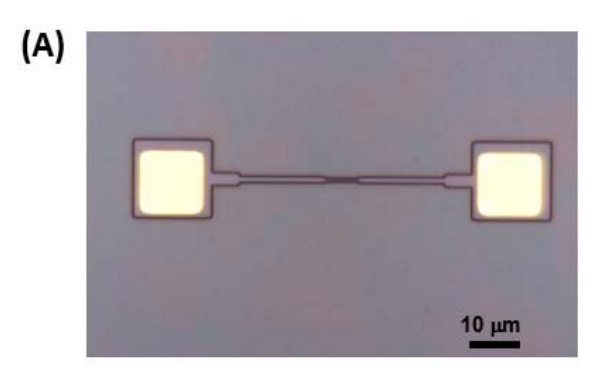
A. Device Fabrication and Characterization

A standard top-down fabrication process had been employed to form n-type and c-axis GaN nanowires on Si (111) substrates [33]–[35]. Then, top contact metallization was deposited on GaN with a deposition sequence of Ti (40 nm)/Al (80 nm)/Ti (40 nm)/Au (40 nm). On the fabricated GaN nanowire surface, the anatase TiO₂ nanoclusters were formed using RF magnetron sputtering at 325 °C with 50 standard cubic centimeters per minute (SCCM) of Ar flow and 300 W RF power [36]. After that, rapid thermal annealing (RTA) was carried out on the devices at 600~700 °C for 30 s to promote ohmic contact formation to nanowires and to induce crystallization of the TiO₂ clusters. Similar fabrication procedures have been followed for making ZnO incorporated GaN NW, and SnO₂ functionalized GaN NW device. For gas sensing measurements the device was placed in a custom designed gas chamber made of stainless steel. A gaseous mixture of NO₂ and compressed breathing air was introduced into the sensing apparatus and the net flow (air $+ NO_2$) was maintained at 100 SCCM. Mass flow controllers (MFCs) independently controlled the flow rate of each component, determining the composition of the mixed gas. The devices were biased with a constant 5 V supply and currents were measured by a National Instrument PXI SMU system. UV illumination to the sensor was applied by a 365 nm light emitting diode. The output power of the UV source was maintained at 470 mW/cm². After the sensor was exposed to NO₂, it had been allowed to regain the baseline current in air at room temperature for 10 mins.

The actual optical image of the proposed GaN nanowire-based sensor device is presented in Figure 1A. It is a lightly doped $0.4\sim0.5~\mu m$ wide GaN two-terminal micro-resistor structure fabricated on silicon substrate and functionalized with a discontinuous layer of photocatalytic metal-oxide nanoclusters. Figure 1B shows FESEM image of the synthesized GaN nanowire positioned between the two metal electrodes. The size of the nanowire sample is observed quite uniform having a height and width of ~400 nm and 400-500 nm, respectively. Since metal-oxide coated GaN NWs are very small in size, reference samples with TiO₂, ZnO, and SnO₂ thin films on sapphire substrate were prepared to obtain Atomic Force Microscopy (AFM) images. The metal-oxides thin films were annealed at 600-700 °C for 30 s expecting that similar metal-oxide morphology has been formed on the substrate as in the metal-oxide coated GaN NW case. The two-dimensional AFM images of the annealed metal-oxides are shown in Figure 2A-C revealing the surface morphologies. The root mean square (rms) surface roughness of TiO₂, ZnO and SnO₂ thin films were obtained as 0.61, 0.67 and 0.85 nm, respectively which indicate the formation of uniform surfaces favorable for gas molecule adsorption.

B. Gas Sensing Properties

The time-dependent NO₂ gas-sensing response–recovery curves of the TiO₂/GaN NW device, ZnO/GaN NW device and SnO₂/GaN NW device were obtained in dry air under UV



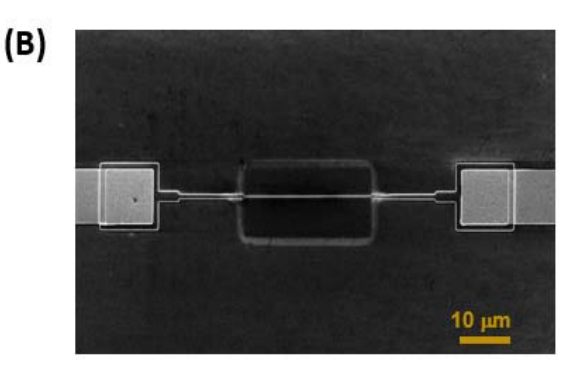


Fig. 1. (A) The optical image showing the top view of the fabricated GaN nanowire-based sensor. (B) FESEM image of the fabricated GaN nanowire.

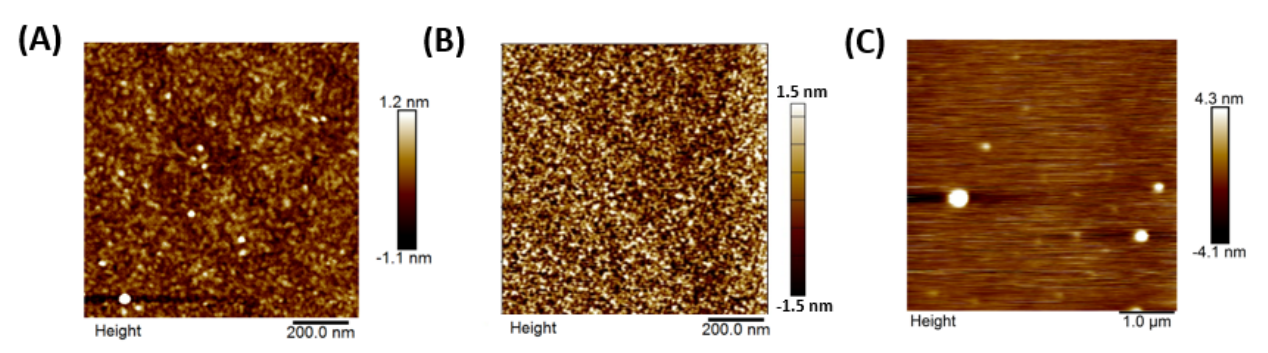
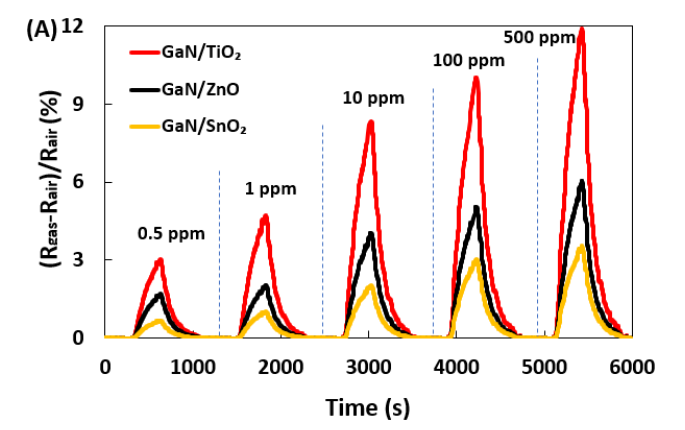


Fig. 2. High-resolution 2D AFM images of the annealed (A) TiO₂ thin film, (B) SnO₂ thin film and (C) ZnO thin film.

light at room temperature (20°). Under the irradiation of UV light, metal-oxide nanocluster photo-desorbs water and oxygen creating surface defect active sites and electron-hole pairs are generated in the GaN backbone. Without UV illumination, the sensor response is degraded due to lack of active-site creation at room temperature. The UV assisted sensing makes it possible to operate the sensor at room-temperature, resulting in a significant reduction in operating power. The measurement was performed by exposing the sensors to various concentrations of NO₂, from 0.5 ppm to 500 ppm as illustrated in Figure 3A. The gas exposure cycle was for 250 s. When gas flow was turned off, the sensors had been allowed to recover in air at room temperature for 10 mins. It is found that the TiO₂/GaN NW device exhibits the highest response among the three synthesized sensor devices, verified from the DFT results as well. Bare GaN nanowire didn't show any significant response toward NO2 gas (not shown). Here, the response has been defined as $(R_{gas} - R_{air})/R_{air}$, where R_{gas} and R_{air} are the resistances of the sensor in the presence of the analyte-air mixture and in the presence of air only, respectively. The base resistance of each GaN/metal-oxide device mainly depends on the charge transfer i.e., depletion region formed in between GaN and metal-oxide. Higher depletion width causes higher base resistance for the device. Here, resistances for the three fabricated devices are observed in $M\Omega$ range and similar in magnitudes. So, this base resistance variation is not expected to cause significant NO₂ response modification in comparison to the sensing surface variation among the metal-oxides. In other words, surface characteristics of the receptor metal-oxides play the key role in determining gas sensing response of the sensor devices, as verified by the DFT simulation study.

Figure 3B plots the responses of the three sensors as a function of NO₂ gas concentration. Each response value plotted



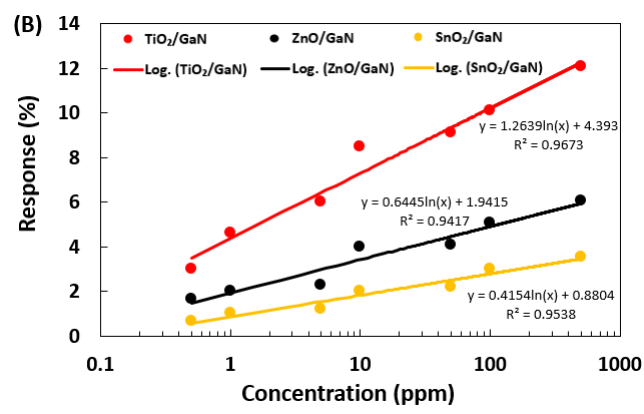


Fig. 3. (A) Percent responses and (B) Function fitting lines of the TiO₂/GaN NW device (red), ZnO/GaN NW device (black) and SnO₂/GaN NW device (yellow) toward varying concentrations of NO₂ gas in dry air under UV light at room temperature (20°C).

is the average response of three consecutive gas exposure responses at the same concentration for the analyte gas. Each sensor was calibrated by setting a reference zero reading

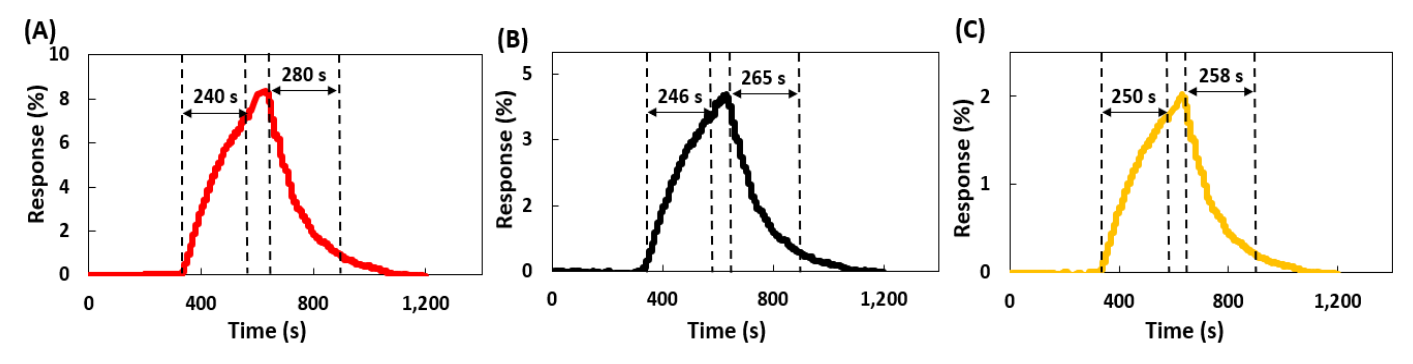


Fig. 4. Response and recovery characteristics of (A) TiO₂/GaN NW device, (B) ZnO/GaN NW device, and (C) SnO₂/GaN NW device exposed to 10 ppm of NO₂ in dry air under UV light at room temperature (20°C).

using pure synthetic air. The fitting equations of the sensor response Y and gas concentration X are represented as Y = $1.263 \ln X + 4.393$, Y = $0.644 \ln X + 1.941$ and Y = $0.415 \ln X + 0.880$ for TiO_2/GaN , ZnO/GaN and SnO_2/GaN sensors, respectively, and the regression coefficient is 0.9673, 0.9417, and 0.9538, respectively. This result indicates that the TiO_2/GaN sensor device exhibits the highest sensitivity and linearity with the logarithm of NO_2 gas concentration among three considered sensors.

Figure 4 shows the gas response-recovery process and response/recovery times of TiO₂/GaN, ZnO/GaN SnO₂/GaN sensors exposed to 10 ppm NO₂ in dry air under UV light at room temperature. The response /recovery time is defined as the time taken by the sensor to achieve 90% of the total response change in the response/recovery stage. It is observed that TiO2/GaN sensor device was the quickest in NO₂ response among the three proposed devices. This finding can be attributed to the stronger chemical interaction between TiO₂ and NO₂ molecules as revealed from the energy and DOS calculations. However, recovery time for the TiO₂/GaN device is found as the longest among all three considered devices. It happens because higher chemical stability of the adsorption system due to larger adsorption energy makes the recovery-process of gas molecules slower. Having lower adsorption energy as well as weaker chemical interaction with NO₂ molecules, SnO₂/GaN device exhibits faster gas recovery than the other two metal-oxide/GaN structures. So, neither very strong nor too weak chemical interaction is desirable between gas and sensor surface in order to achieve a rapid response-recovery process.

III. COMPUTATIONAL METHODS AND MODEL SYSTEMS A. Computational Methods

All the first-principles calculations within density functional theory (DFT) in the Kohn-Sham approach [37] have been performed using BURAI 1.3, a GUI of Quantum Espresso. This GUI system is developed as JavaFX application, and requires Java Runtime Environment (JRE). As an exchange-correlation energy functional approximation, the generalized gradient approximation (GGA) in the Perdew–Burke–Ernzerhof form (PBE) has been utilized [38]. Ultra-soft pseudopotentials have been used with non-linear core correction having a cutoff for wavefunctions and charge

density of 51 Ry and 575 Ry, respectively. The convergence criteria of the self-consistent field (SCF) electronic optimization was set to the value of 1.0×10^{-6} Ry with a non-polarized spin. A symmetric fermi vacuum k-point mesh of $10 \times 10 \times 1$ has been applied in the calculations associated with the electronic density of states (DOS). Gaussian smearing was set as fermi vacuum occupations with a smearing width of 1.0×10^{-2} Ry. The optimized structures for the surface with adsorbate were obtained by placing the NO₂ gas molecule \sim 3 Å above the surface and optimizing the systems using the Broyden-Fletcher-Goldfarb-Shanno (BFGS) algorithm [39]. All the atomic positions were fully relaxed until the forces on each atom were less than 1.0×10^{-3} Ry/Bohr and energy was less than 1.0×10^{-4} Ry. All the calculations were performed at 293K and no UV irradiation effect was considered. The adsorption energy of gas molecules adsorbed on the GaN/metal-oxide nanocomposites were computed using the following formula: $E_{adsorption} = E_{(GaN/metal-oxide+NO2)} E_{GaN/metal-oxide} - E_{NO2}$; where $E_{(GaN/metal-oxide+NO2)}$ is the total energy of the adsorption system, E_{GaN/metal-oxide} is the energy of the GaN/metal-oxide nanocomposite, and E_{NO2} is the energy of isolated NO₂ gas molecules. The adsorption energies of stable configurations are negative. The more negative the adsorption energy, the more energy favorable the adsorption system, i.e., the stronger the interaction of adsorbate with the nanocomposite.

B. Model Systems

The unit cells used in the nanocomposite design, such as-GaN (wurtzite), TiO₂ (anatase), ZnO (wurtzite) and SnO₂ (cassiterite) were taken from "American Mineralogists Database" webpage which were reported by Wyckoff [40]. For GaN/TiO₂ nanostructure simulation, a 2 × 1 × 1 supercell was considered containing a total of 51 Atoms (11 Ga, 21 N, 7 Ti and 12 O atoms). Similar supercells were chosen for GaN/ZnO and GaN/SnO₂ nanostructure simulation having 47 (8 Ga, 15 N, 14 Zn and 10 O atoms) and 53 (16 Ga, 20 N, 8 Sn and 9 O atoms) atoms, respectively. All atoms of the considered nanocomposites had been allowed to relax. The interface between materials can't be formed directly in the BURAI GUI of Quantum Espresso. So, QuantumWise ATK build property had been used to form the interfaces between GaN and metaloxides. The designed nanocomposites had been transferred

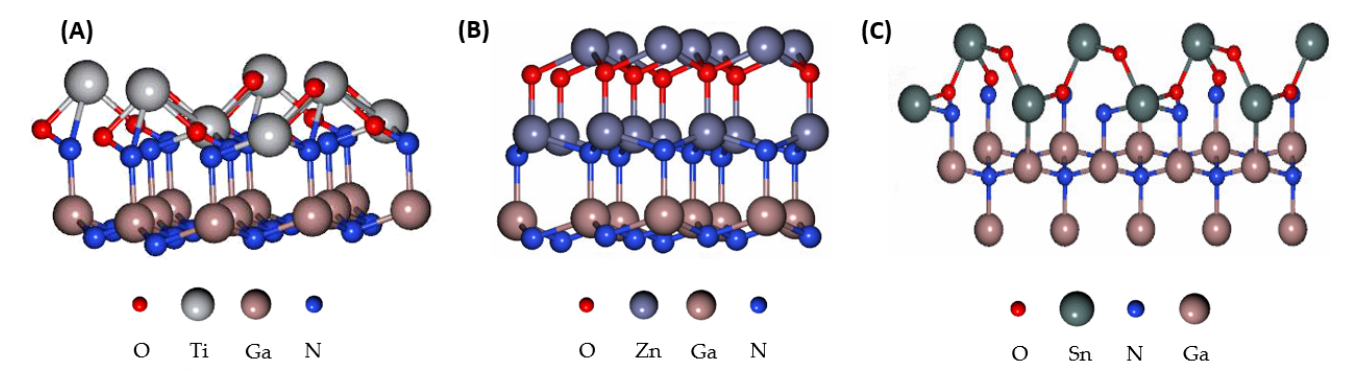


Fig. 5. Optimized geometry of (A) GaN/TiO₂ nanocomposite, (B) GaN/ZnO nanocomposite, and (C) GaN/SnO₂ nanocomposite. The gray spheres are Ti atoms and the red and blue ones represent O and N atoms, respectively. The brown, light blue and green spheres denote Ga, Zn and Sn atoms, respectively.

to Quantum Espresso for further DFT calculations. Though c-plane GaN is generally terminated by Ga atoms, N atoms were found to be present within the interface of the optimized and stable structures.

The anatase TiO2 nanoparticle model possess two types of titanium atoms, referred to as five-fold (5f-Ti) and six-fold (6f-Ti), as well as two types of oxygen atoms, specified by three-fold (3f-O) and two-fold (2f-O) O atoms [41]. Generally, the 2f-O and 5f-Ti atoms are more reactive than the 3f-O and 6f-Ti atoms because of their unsaturated coordination. The optimized structure of the GaN/TiO₂ nanocomposite is displayed in Figure 5A. Each Zn and O atom at the surface of the monolayer wurtzite ZnO is threefold coordinated, and, thus, exhibits an unsaturated bond which allows for strong interaction with gas molecules. The optimized structure of the GaN/ZnO nanocomposite is displayed in Figure 5B. Similarly, unsaturated Sn atoms on the SnO₂ surface act as suitable places for the adsorption of target gas molecules. The optimized structure of the GaN/SnO₂ nanocomposite is displayed in Figure 5C. It is well known that NO₂ molecule has a bent structure. The N-O bond length and corresponding O-N-O bond angle of NO₂ molecule have been estimated to be 1.20 A° and 134.3°, respectively.

The metal-oxide/GaN molecular models are designed to investigate the chemical interaction of NO₂ molecule with the sensor surfaces. Here, the characteristics of the interacting molecules are mainly influenced by the neighboring atoms. Even though the device models don't have actual dimensions, adsorption properties and overlapping density of states between NO₂ molecule and sensor surface are close to experimental values [42].

IV. SIMULATION RESULTS AND DISCUSSION A. Adsorption of NO₂ Molecule on GaN/Metal-Oxide Nanocomposites

For each of the GaN/metal-oxide nano- composites, multiple adsorption configurations were considered. The most stable adsorption configuration structures of the nanocomposites after NO₂ molecule adsorption are displayed in Figure 6A-C. Fivefold coordinated titanium atom (5f-Ti) is well established as the catalytic active site of TiO₂ for NO₂ gas adsorption reaction. The results from the geometry optimization process

indicate that the N-O bonds of the adsorbed NO₂ molecule are stretched after the adsorption on TiO₂ surface of the nanocomposite. This happens due to the transference of electronic density from the Ti-O (TiO₂) and N-O (NO₂) bonds to the interaction site between Ti of TiO₂ and O of NO₂ molecule. Moreover, the O-N-O bond angle of the NO₂ molecule after the adsorption on the nanocomposite was decreased due to the weakening of the N-O bonds of NO₂ molecule [43]. This adsorption process also increases the 'p' characteristics of bonding molecular orbitals so that the sp^2 hybridization of nitrogen in the NO₂ molecule becomes $near-sp^3$ [44].

Upon adsorption on GaN/ZnO nanocomposite, the NO₂ molecule was observed to be slightly distorted with respect to the gas phase geometry being the N-O bond elongated by 0.07-0.09 Å and the bond angle contracted by 6.3°. The bond length and bond angle distortion of NO₂ molecule on ZnO/GaN surface were found much less than that on TiO₂/GaN surface. In case of molecular interaction in GaN/SnO₂-NO₂ adsorption complex, the N-O bond elongation and angle contraction were calculated as 0.06-0.1 Å and 8°, respectively which are very close to the values obtained for GaN/ZnO-NO₂ adsorption complex.

The self-consistent field (SCF) calculations were performed and converged for the three considered nanocomposites with and without NO₂ molecule. The adsorption energies were calculated as -2.31 eV, -1.96 eV and -1.95 eV for the GaN/TiO₂-NO₂, GaN/ZnO-NO₂ and GaN/SnO₂-NO₂ adsorption complexes, respectively. The results indicate that GaN/TiO₂ surface provides the most energy favorable and stable NO₂ adsorption in comparison with the other two nanocomposites, making it the most likely binding site of NO₂ gas molecules. This explains the fact of GaN/TiO₂ device being quicker in NO₂ response with a slower recovery process. The bond lengths, bond angles and adsorption energies for the three considered adsorption complexes are summarized in Table I.

B. Electronic Structures

Density of states (DOS) is defined as the number of allowed electron (or hole) states per volume at a given energy. Charge carrier transport phenomena of conductive solids largely depend on this parameter. In order to further

TABLE I

BOND LENGTHS (Å) AND BOND ANGLES (DEGREES) OF NO₂ MOLECULE ADSORBED ON GaN/METAL-OXIDE NANOCOMPOSITES WITH ADSORPTION ENERGIES (eV)

Type of complex	N-O1 (Å)	N-O2 (Å)	O–N–O angle (degree)	Adsorption energy (eV)
Before adsorption	1.20	1.20	134.3	-
GaN/TiO ₂ -NO ₂	1.30	1.33	119	-2.31
GaN/ZnO-NO ₂	1.27	1.297	128	-1.96
GaN/SnO ₂ -NO ₂	1.26	1.30	126	-1.95

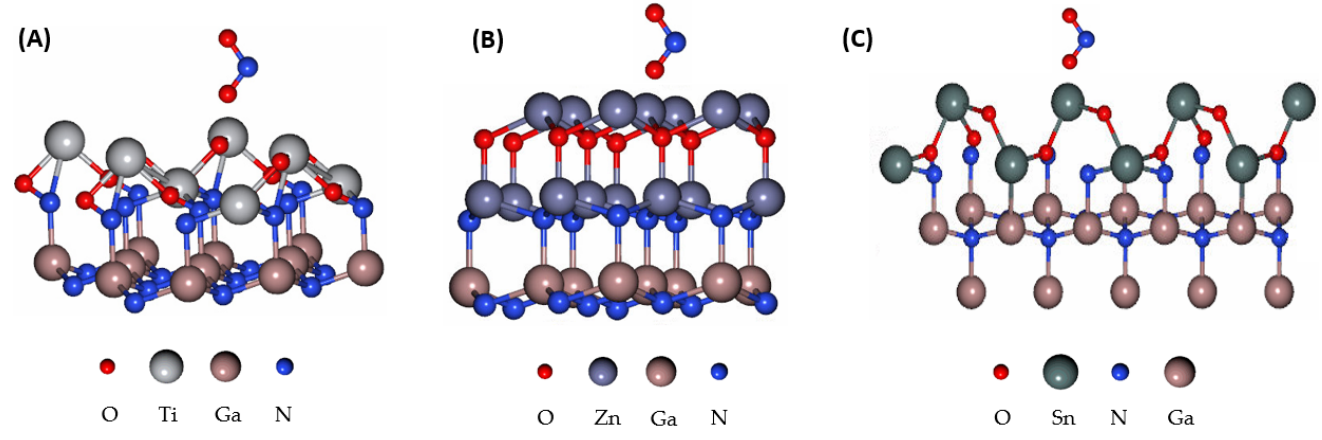


Fig. 6. Side views of the most stable adsorption configurations of NO₂ on (A) GaN/TiO₂ nanocomposite, (B) GaN/ZnO nanocomposite, and (C) GaN/SnO₂ nanocomposite. The gray spheres are Ti atoms and the red and blue ones represent O and N atoms, respectively. The brown, light blue and green spheres denote Ga, Zn and Sn atoms, respectively.

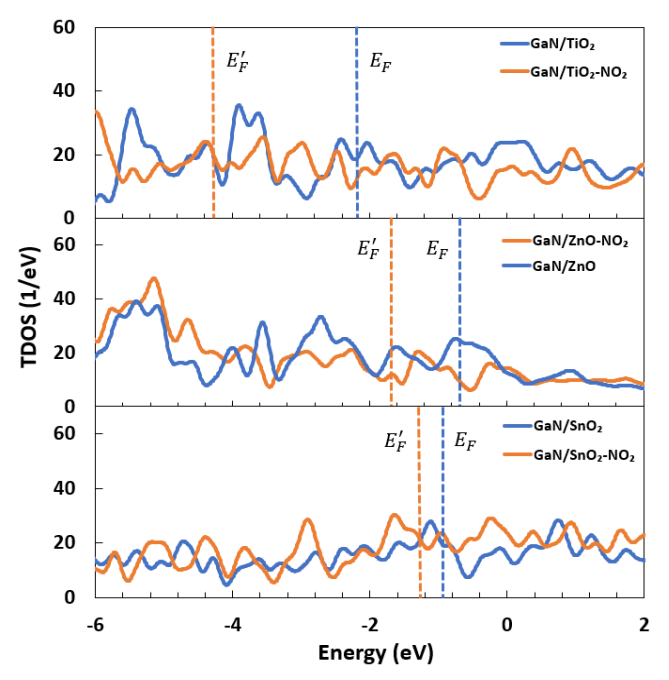


Fig. 7. Total density of states (TDOS) for GaN/TiO₂ nanocomposite, GaN/ZnO nanocomposite, and GaN/SnO₂ nanocomposite before and after the NO₂ adsorption process. E_F and E_F' denote Fermi energies of the nanocomposite before and after the NO₂ adsorption, respectively.

study NO₂ adsorption on the GaN/metal-oxide nano- composites, the total and projected density of states for the considered adsorption configurations were analyzed. Figure 7

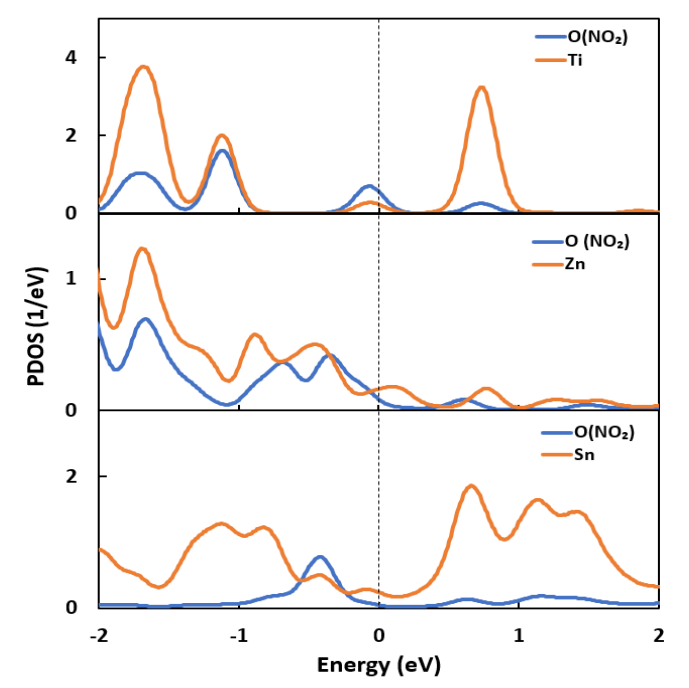


Fig. 8. Projected density of states (PDOS) for the adsorption complexes of NO₂ molecule with GaN/ TiO₂, GaN/ZnO and GaN/SnO₂ nanocomposites. Fermi energies (E_F') of the adsorption complexes have been shifted to zero.

presents the total density of states (TDOS) for GaN/metaloxide nanocomposites before and after the adsorption process. Fermi level shifts toward lower energy have been observed

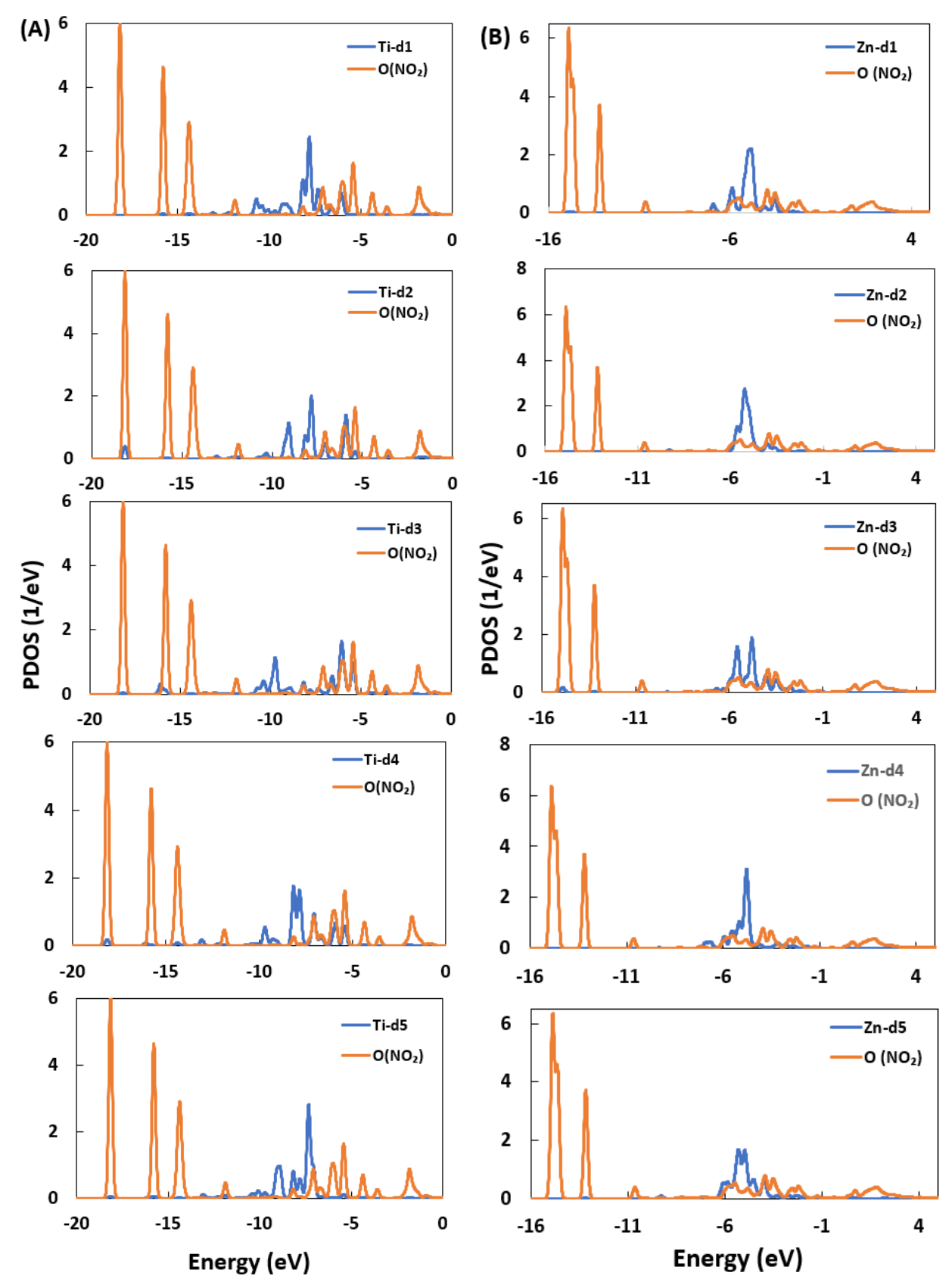


Fig. 9. PDOSs of the O atom of NO₂ molecule with different d orbitals of the (A) Ti atom of GaN/TiO₂ nanocomposite and (B) Zn atom of GaN/ZnO nanocomposite.

for all the three nanocomposites, confirming the electron withdrawing nature of NO_2 molecule. It is found that the Fermi energy (E_F) is shifted from -2.210 eV to -4.293 eV due to

adsorption on GaN/TiO_2 structure. This is the largest E_F shift (2.08 eV) among the three considered nanocomposites. ZnO and SnO_2 nanocomposites showed an E_F shift of 0.97 eV

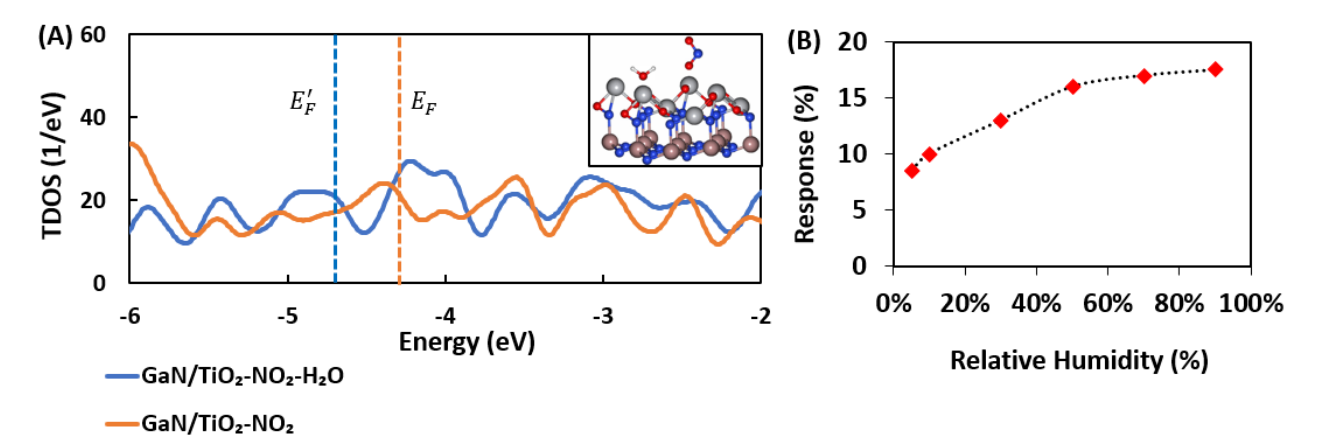


Fig. 10. (A) Total density of states (TDOS) for GaN/TiO_2 - NO_2 adsorption complex in the presence of water molecule (blue) and in the absence of water molecule (orange). Inset shows the adsorption complex of NO_2 and H_2O molecules on GaN/TiO_2 nanocomposite. The gray spheres are Ti atoms and the red and blue ones represent O and N atoms, respectively. The brown and white spheres denote Ga and H atoms, respectively. E_F and E_F' denote Fermi energies of the nanocomposite without and with the H_2O molecule, respectively. (B) Responses of GaN/TiO_2 NW based sensor to 10 ppm of NO_2 gas under UV at 20 °C for different humid conditions.

(−0.65 to −1.62 eV) and 0.30 eV (−0.96 to −1.26 eV), respectively. The alteration of Fermi energy indicates the change in charge carrier concentration which results into the modification of conductivity within the nanocomposite. That means, GaN/TiO₂ nanostructure is expected to undergo higher conductivity change than the other two nanostructures upon NO₂ gas molecule exposure. The TDOS of all three nanocomposite-gas complexes show significant differences in comparison with the non-adsorbed nano- composites. These differences include shifting of energies of the peaks and creating some additional peaks in the DOS of the considered systems. These changes in the states near Fermi energy would influence the electronic transport properties of the nanocomposites.

The projected density of states (PDOS) for the adsorption complexes of NO2 molecule with metal-oxide/GaN nanocomposites have been displayed in Figure 8. Fermi energies (E'_F) of the adsorption complexes have been shifted to common zero for a better comparison. The PDOS of the oxygen atom of NO₂ molecule is presented with the PDOS of Ti, Zn and Sn atom from the nanocomposite adsorption systems, respectively. The O of NO₂ shows significant PDOS overlaps with metal atoms of the metal-oxides within valence band. These overlaps in the PDOSs suggest the tendency of formation of chemical bonds between the concerned atoms by hybridization which is a measure of effective interaction of NO₂ molecule with the respective metal-oxide/GaN surfaces. Near the Fermi energy, O of NO₂ exhibits the largest PDOS overlap with Ti of TiO₂ among the three PDOS overlaps and contributes noteworthy energy states. In consequence, a substantial modification of electronic transport behavior can be expected within GaN/TiO₂ nanostructure at NO₂ gas exposure. Therefore, the obtained DFT calculation results corroborates our experimental data.

Figure 9 displays the PDOSs of the oxygen atom of NO_2 molecule with different d orbitals of the titanium atom and zinc atom respectively. As can be seen from this figure, the PDOSs of the oxygen atom of NO_2 molecule and d4 orbital of the titanium atom show large overlaps in some energy values. Though

the energy of all five 3d orbitals is equivalent, different shapes of the orbitals causes different PDOS overlaps. In case of Zn atom of ZnO/GaN nanocomposite, d3 orbital shows largest overlap with O-atom of NO₂ as illustrated in Figure 9B. However, Sn atom on the SnO₂/GaN nanocomposite surface interacts with O-atom of NO₂ through Sn-s and p orbitals (not shown). Sn-d orbitals show no significant overlap. The overall PDOS results suggest the occurrence of chemisorption between NO₂ molecule and the considered GaN/metal-oxide nanocomposites.

C. Effect of Humidity on Adsorbate-Nanocomposite Interaction

In order to simulate the environmental humidity effect on the NO₂ adsorption process by the GaN/metal-oxide nanocomposites, H₂O molecule was placed along with NO₂ molecule on top of the GaN/TiO₂ nanocomposite in DFT calculations (Inset of Figure 10). In this case, only GaN/TiO₂ nanostructure was chosen since it exhibited better NO₂ adsorption properties than other two considered nanocomposites in both DFT calculations and experimental results. It is found that adsorption energy for the GaN/TiO₂-NO₂ adsorption complex got more negative (-3.9 eV) in the presence of H_2O molecule. This means, the GaN/TiO₂ nanocomposite becomes more energy favorable and chemically stable for NO2 adsorption at higher humid conditions. This phenomenon is attributed to the fact that water molecule introduces additional electron cloud in the nanocomposite. Since NO₂ is highly electrophilic in nature, it exhibits stronger electronic interaction in the presence of additional electron cloud.

TDOS data in Figure 10A reveals that Fermi energy is further shifted from -4.293 eV to -4.74 eV due to H_2O adsorption, confirming the alteration in electronic transport properties. Therefore, the conductivity of the GaN/TiO₂ nanocomposite is expected to be modified due to the inclusion of water molecule. However, analyte recovery process of the nanocomposite may be degraded due to excessive chemical stability at higher humid conditions. Furthermore,

the simulation of NO₂ adsorption on sensor surface has been performed by taking into consideration the presence of oxygen (dry air) and oxygen/hydroxyl groups (wet air). It is found that fermi-energy shift is larger in wet air condition than in dry air, indicating an increase in gas response in presence of hydroxyl groups (Supporting Information).

In order to verify the results obtained from DFT calculations, the synthesized GaN/TiO2NW based sensor was exposed to different environmental humidity conditions at room temperature (20°). Bronkhorst Controlled Evaporator and Mixer (CEM) has been used as the core component for environmental humidity generation and control. The sensor device was exposed to 10 ppm of NO2 gas at relative humidity conditions ranging from 5% RH to 90% RH. It was observed that the response was enhanced with increasing humid conditions initially and saturates at high humidity as illustrated in Figure 10B. The fact of increasing senor response with the increasing humidity strongly supports the lower energy shift of Fermi level from the TDOS results. However, the gas recovery-process was degraded at elevated RH due to excessive chemical stability as expected from the DFT energy calculations. It was found from our previous research that sensor baseline resistance of GaN/metal-oxide device is altered due to humidity variation. Therefore, apart from the baseline variation, gas response magnitudes of the sensors are found quite robust against significant humidity variations.

V. CONCLUSION

Research and development of chemical sensor devices continue to be faced with numerous challenges in terms of sensitivity, selectivity, promptness of response, robustness, and many other aspects. Semiconducting GaN is one of the promising materials which has been exploited to address those short comings in sensing applications. This paper reports that TiO₂ functionalized GaN nanowire has shown better adsorption behaviors and sensing response toward NO₂ gas compared to ZnO and SnO₂ functionalized GaN sensors. Furthermore, higher humid conditions enhance gas sensing responses of the GaN/TiO₂ device with a slight degradation in recovery-process. This simulation and experimental comparative study will shine light on the analysis and selection of suitable metal-oxide catalyst in GaN nanostructures-based chemical sensors for current and future researchers.

ACKNOWLEDGMENT

The metal-oxide/GaN nanowire based NO₂ gas sensing devices were fabricated in the Nanofab of the NIST Center for Nanoscale Science and Technology. Gas sensing measurements were conducted at N5 Sensors, Inc.

CONFLICTS OF INTEREST

The authors declare no conflict of interest.

REFERENCES

 H. Song and S. Lee, "Red light emitting solid state hybrid quantum dot-near-UV GaN LED devices," *Nanotechnology*, vol. 18, no. 25, May 2007, Art. no. 255202, doi: 10.1088/0957-4484/18/25/255202.

- [2] Y. Ikawa, K. Lee, J.-P. Ao, and Y. Ohno, "Two-dimensional device simulation of AlGaN/GaN heterojunction FET side-gating effect," *Jpn. J. Appl. Phys.*, vol. 53, no. 11, Oct. 2014, Art. no. 114302, doi: 10.7567/JJAP.53.114302.
- [3] A. Podolska, R. M. Seeber, U. K. Mishra, K. D. G. Pfleger, G. Parish, and B. D. Nener, "Detection of biological reactions by AlGaN/GaN biosensor," in *Proc. COMMAD*, Melbourne, VIC, Australia, Dec. 2012, pp. 75–76, doi: 10.1109/COMMAD.2012.6472367.
- [4] N. Prokopuk, K.-A. Son, T. George, and J. S. Moon, "Development of GaN-based micro chemical sensor nodes," in *Proc. IEEE SENSORS*, Irvine, CA, USA, Nov. 2005, pp. 199–202, doi: 10.1109/ICSENS.2005.1597670.
- [5] A. M. Nahhas, "Review of GaN nanostructured based devices," Amer. J. Nanomaterials, vol. 6, no. 1, pp. 1–14, May 2018, doi: 10.12691/ajn-6-1-1
- [6] Z. L. Wang, "Novel nanostructures and nanodevices of ZnO," in *Zinc Oxide Bulk, Thin Films and Nanostructures*, Amsterdam, The Netherlands: Elsevier, 2006, pp. 339–370.
- [7] I. S. Elashmawi, A. M. Abdelghany, and N. A. Hakeem, "Quantum confinement effect of CdS nanoparticles dispersed within PVP/PVA nanocomposites," *J. Mater. Sci., Mater. Electron.*, vol. 24, no. 8, pp. 2956–2961, Mar. 2013, doi: 10.1007/s10854-013-1197-z.
- [8] D. Li et al., "Realization of a high-performance GaN UV detector by nanoplasmonic enhancement," Adv. Mater., vol. 24, no. 6, pp. 845–849, Jan. 2012, doi: 10.1002/adma.201102585.
- [9] Y.-F. Sun et al., "Metal oxide nanostructures and their gas sensing properties: A review," Sensors, vol. 12, no. 3, pp. 2610–2631, Feb. 2012, doi: 10.3390/s120302610.
- [10] J. Ree, Y. H. Kim, and H. K. Shin, "Dynamics of gas-surface interactions: Reaction of atomic oxygen with chemisorbed hydrogen on tungsten," *J. Phys. Chem. A*, vol. 101, no. 25, pp. 4523–4534, Jun. 1997, doi: 10.1021/jp9706994.
- [11] J. Zhang, X. Liu, G. Neri, and N. Pinna, "Nanostructured materials for room-temperature gas sensors," *Adv. Mater.*, vol. 28, no. 5, pp. 795–831, Dec. 2015, doi: 10.1002/adma.201503825.
- [12] N. Joshi, T. Hayasaka, Y. Liu, H. Liu, O. N. Oliveira, and L. Lin, "A review on chemiresistive room temperature gas sensors based on metal oxide nanostructures, graphene and 2D transition metal dichalcogenides," *Microchimica Acta*, vol. 185, no. 4, p. 213, Mar. 2018, doi: 10.1007/s00604-018-2750-5.
- [13] X. Liu, T. Ma, N. Pinna, and J. Zhang, "Two-dimensional nanostructured materials for gas sensing," *Adv. Funct. Mater.*, vol. 27, no. 37, Aug. 2017, Art. no. 1702168, doi: 10.1002/adfm.201702168.
- [14] M. A. H. Khan, B. Thomson, R. Debnath, A. Motayed, and M. V. Rao, "Nanowire-based sensor array for detection of cross-sensitive gases using PCA and machine learning algorithms," *IEEE Sensors J.*, to be published, doi: 10.1109/JSEN.2020.2972542.
- [15] A. Rani, K. DiCamillo, M. A. H. Khan, M. Paranjape, and M. E. Zaghloul, "Tuning the polarity of MoTe₂ FETs by varying the channel thickness for gas-sensing applications," *Sensors*, vol. 19, no. 11, p. 2551, Jun. 2019, doi: 10.3390/s19112551.
- [16] M. A. H. Khan, R. Debnath, A. Motayed, and M. V. Rao, "Back-gate GaN nanowire-based FET device for enhancing gas selectivity at room temperature," *Jpn. J. Appl. Phys.*, submitted for publication.
- [17] G. S. Aluri et al., "Highly selective GaN-nanowire/TiO₂-nanocluster hybrid sensors for detection of benzene and related environment pollutants," *Nanotechnology*, vol. 22, no. 29, Jun. 2011, Art. no. 295503, doi: 10.1088/0957-4484/22/29/295503.
- [18] S. R. Morrison, "Selectivity in semiconductor gas sensors," Sens. Actuators B, Chem., vol. 12, no. 4, pp. 425–440, 1987, doi: 10.1016/0250-6874(87)80061-6.
- [19] P. A. Sermon and G. C. Bond, "Hydrogen spillover," *Catal. Rev.*, vol. 8, no. 1, pp. 211–239, Jan. 1974, doi: 10.1080/01614947408071861.
- [20] A. Fujishima and K. Honda, "Electrochemical photolysis of water at a semiconductor electrode," *Nature*, vol. 238, no. 5358, pp. 37–38, Jul. 1972, doi: 10.1038/238037a0.
- [21] Y. H. Navale et al., "Zinc oxide hierarchical nanostructures as potential NO₂ sensors," Sens. Actuators B, Chem., vol. 251, pp. 551–563, Nov. 2017, doi: 10.1016/j.snb.2017.05.085.
- [22] Y. J. Kwon, S. Y. Kang, P. Wu, Y. Peng, S. S. Kim, and H. W. Kim, "Selective improvement of NO₂ gas sensing behavior in SnO₂ nanowires by ion-beam irradiation," ACS Appl. Mater. Interfaces, vol. 8, no. 21, pp. 13646–13658, May 2016, doi: 10.1021/acsami.6b01619.
- [23] J. S. Symanski and S. Bruckenstein, "Conductometric sensor for parts per billion sulfur dioxide determination," *Anal. Chem.*, vol. 58, no. 8, pp. 1771–1777, May 2002, doi: 10.1021/ac00121a038.

- [24] M. Khan, M. Rao, and Q. Li, "Recent advances in electrochemical sensors for detecting toxic gases: NO₂, SO₂ and H₂S," *Sensors*, vol. 19, no. 4, p. 905, Feb. 2019, doi: 10.3390/s19040905.
- [25] S. C. Anenberg et al., "Impacts and mitigation of excess diesel-related NOx emissions in 11 major vehicle markets," *Nature*, vol. 545, no. 7655, pp. 467–471, May 2017, doi: 10.1038/nature22086.
- [26] J. S. M. Boleij *et al.*, "Domestic air pollution from biomass burning in Kenya," *Atmos. Environ.*, vol. 23, no. 8, pp. 1677–1681, Jan. 1989, doi: 10.1016/0004-6981(89)90052-8.
- [27] E. Robinson and R. C. Robbins, "Gaseous nitrogen compound pollutants from urban and natural sources," *J. Air Pollut. Control Assoc.*, vol. 20, no. 5, pp. 303–306, Mar. 2012, doi: 10.1080/00022470.1970.10469405.
- [28] R. Ehrlich, "Effect of nitrogen dioxide on resistance to respiratory infection," *Bacteriolog. Rev.*, vol. 30, no. 3, pp. 604–614, 1966.
- [29] S. Genc, Z. Zadeoglulari, S. H. Fuss, and K. Genc, "The adverse effects of air pollution on the nervous system," *J. Toxicol.*, vol. 2012, pp. 1–23, Feb. 2012, doi: 10.1155/2012/782462.
- [30] Y. Yong, X. Su, H. Cui, Q. Zhou, Y. Kuang, and X. Li, "Two-dimensional tetragonal GaN as potential molecule sensors for NO and NO₂ detection: A first-principle study," ACS Omega, vol. 2, no. 12, pp. 8888–8895, Dec. 2017, doi: 10.1021/acsomega.7b01586.
- [31] Y. Yong, H. Jiang, X. Li, S. Lv, and J. Cao, "The cluster-assembled nanowires based on M₁₂N₁₂ (M = Al and Ga) clusters as potential gas sensors for CO, NO, and NO₂ detection," *Phys. Chem. Chem. Phys.*, vol. 18, no. 31, pp. 21431–21441, 2016, doi: 10.1039/C6CP02931K.
- [32] Y. Yong, H. Cui, Q. Zhou, X. Su, Y. Kuang, and X. Li, "Adsorption of gas molecules on a graphitic GaN sheet and its implications for molecule sensors," *RSC Adv.*, vol. 7, no. 80, pp. 51027–51035, 2017, doi: 10.1039/C7RA11106A.
- [33] D. Paramanik et al., "Formation of large-area GaN nanostructures with controlled geometry and morphology using top-down fabrication scheme," J. Vac. Sci. Technol. B, Nanotechnol. Microelectron., Mater., Process., Meas., Phenomena, vol. 30, no. 5, Sep. 2012, Art. no. 052202, doi: 10.1116/1.4739424.
- [34] M. A. H. Khan, B. Thomson, R. Debnath, A. Rani, A. Motayed, and M. V. Rao, "Reliable anatase-titania nanoclusters functionalized GaN sensor devices for UV assisted NO₂ gas-sensing in ppb level," *Nanotechnology*, vol. 31, no. 15, Jan. 2020, Art. no. 155504, doi: 10.1088/1361-6528/ab6685.
- [35] C. Shi et al., "High-performance room-temperature TiO₂-functionalized GaN nanowire gas sensors," Appl. Phys. Lett., vol. 115, no. 12, Sep. 2019, Art. no. 121602, doi: 10.1063/1.5116677.
- [36] G. S. Aluri et al., "Methanol, ethanol and hydrogen sensing using metal oxide and metal (TiO₂-Pt) composite nanoclusters on GaN nanowires: A new route towards tailoring the selectivity of nanowire /nanocluster chemical sensors," *Nanotechnology*, vol. 23, no. 17, 2012, Art. no. 175501, doi: 10.1088/09574484/23/17/175501.
- [37] W. Kohn and L. J. Sham, "Self-consistent equations including exchange and correlation effects," *Phys. Rev.*, vol. 140, no. 4A, pp. A1133–A1138, Nov. 1965, doi: 10.1103/PhysRev.140.A1133.
- [38] J. P. Perdew, K. Burke, and M. Ernzerhof, "Generalized gradient approximation made simple," *Phys. Rev. Lett.*, vol. 78, no. 7, p. 1396, Feb. 1997, doi: 10.1103/PhysRevLett.78.1396.
- [39] M. F. Møller, "A scaled conjugate gradient algorithm for fast supervised learning," *Neural Netw.*, vol. 6, no. 4, pp. 525–533, Nov. 1993, doi: 10.7146/dpb.v19i339.6570.
- [40] R. W. G. Wyckoff, Crystal Structures, 2nd ed. New York, NY, USA: Interscience, 1972.
- [41] J. Liu, Q. Liu, P. Fang, C. Pan, and W. Xiao, "First principles study of the adsorption of a NO molecule on N-doped anatase nanoparticles," *Appl. Surf. Sci.*, vol. 258, no. 20, pp. 8312–8318, Aug. 2012, doi: 10.1016/j.apsusc.2012.05.053.
- [42] R. Ponnusamy et al., "Experimental and density functional theory investigations of catechol sensing properties of ZnO/RGO nanocomposites," Appl. Surf. Sci., vol. 495, Nov. 2019, Art. no. 143588, doi: 10.1016/j.apsusc.2019.143588.
- [43] J. Liu, L. Dong, W. Guo, T. Liang, and W. Lai, "CO adsorption and oxidation on N-Doped TiO₂ nanoparticles," *J. Phys. Chem. C*, vol. 117, no. 25, pp. 13037–13044, Jun. 2013, doi: 10.1021/jp4001972.
- [44] A. Abbasi, J. J. Sardroodi, and R. Ebrahimzadeh, "TiO₂/gold nanocomposite as an extremely sensitive molecule sensor for NO₂ detection: A DFT study," *J. Water Environ. Nanotechnol.*, vol. 1, no. 1, pp. 55–62, 2016.

Md Ashfaque Hossain Khan received the B.Sc. degree in electrical and electronic engineering from the Bangladesh University of Engineering and Technology, Dhaka, Bangladesh, in 2015, and the M.S. degree in electrical engineering from George Mason University, Fairfax, VA, USA, where he is currently pursuing the Ph.D. degree in electrical engineering. He has been working as a Guest Researcher with the Nanofab of the NIST Center for Nanoscale Science and Technology since 2018. His current research interests include simulation, fabrication, and characterization of semiconducting nanowire-based electrical devices for chemical/gas sensing.

Brian Thomson received the bachelor's degree in chemical engineering and the master's degree in technical entrepreneurship and management from the University of Rochester in 2011 and 2012, respectively. He is a Senior Product Engineer with N5 Sensors. He is responsible for managing gas sensor testing, integration, and product development.

Abhishek Motayed received the Ph.D. degree from the Electrical and Computer Engineering Department, University of Maryland, College Park, in 2007. During his graduate studies, he worked at the National Institute of Standards and Technology (NIST) as a Guest Scientist. Dr. Motayed continued working at NIST after graduating, with an appointment as a Research Scientist at the Institute of Research in Electronics and Applied Physics, University of Maryland. He is currently the CEO of N5 Sensors, Inc., Rockville, MD, USA. His current research expertise and interests are high-performance nanoscale electronic/optical devices with emphasis on large-scale integration, novel chemical/biological/radiation sensor systems, energy conversion/storage, and bio-medical applications of nanoscale devices.

Qiliang Li received the Ph.D. degree in electrical and computer engineering from North Carolina State University in 2004. His doctoral research was in the area of molecular electronics and hybrid silicon/molecular field effect transistors and memories. In October 2004, he joined the Semiconductor Electronics Division, National Institute of Standards and Technology (NIST), Gaithersburg, MD, USA, as a Research Scientist, where he was involved with the fabrication, characterization, and simulation of CMOS and nanoelectronics materials and devices. He joined the faculty of George Mason University as an Assistant Professor of Electrical and Computer Engineering in 2007 and promoted to an Associate Professor in 2012. He has worked on molecular electronics, nanoelectronics, solar cell, ferroelectric memory, and magnetoresistance devices. He has authored or coauthored more than 60 technical articles and holds two U.S. patents. He received the honor of Virginia Microelectronics Consortium Professorship in 2007. He received the NSF CAREER Award in 2009, the Mason Emerging Researcher/Scholar/Creator Award in 2011, and the VSE Rising Star Award in 2011.

Mulpuri V. Rao received the B.Tech. degree in electronics and communication engineering from the College of Engineering, Kakinada, India, in 1977, the M.Tech. degree in material science from the Indian Institute of Technology Bombay, Mumbai, India, in 1979, and the M.S. and Ph.D. degrees in electrical engineering from Oregon State University, Corvallis, in 1983 and 1985, respectively. From 1979 to 1981, he was a Lecturer in electronics and communication engineering with the Sidhartha Engineering College, Vijayawada, India. Since August 1984, he has been with George Mason University, Fairfax, VA, USA, where he is currently a Professor with the Electrical and Computer Engineering Department. He is the author or coauthor of more than 120 articles published in various journals in the areas of epitaxial growth, ion implantation, ohmic contacts, material characterization, photodetectors, microwave and high-power devices, microfluidic cells, and gas sensing.